

Evaluation of cytotoxic effect of siphonochilone from African ginger: an *in vitro* analysis

Alba Ortigosa-Palomo^{1,2,3} | David Fuentes-Ríos⁴ | Francisco Quiñonero^{1,3} |
 Consolación Melguizo^{1,2,3} | Raul Ortiz^{1,2,3}  | Juan M. López-Romero⁴ |
 Jose Prados^{1,2,3}

¹Institute of Biopathology and Regenerative Medicine (IBIMER), Center of Biomedical Research (CIBM), University of Granada, Granada, Spain

²Department of Anatomy and Embryology, Faculty of Medicine, University of Granada, Granada, Spain

³Instituto de Investigación Biosanitaria ibs. Granada, Granada, Spain

⁴Department of Organic Chemistry, Faculty of Sciences, University of Malaga, Málaga, Spain

Correspondence

Raul Ortiz and Consolación Melguizo, Institute of Biopathology and Regenerative Medicine (IBIMER), Center of Biomedical Research (CIBM), University of Granada, Granada 18100, Spain.

Email: roquesa@ugr.es and melguizo@ugr.es

Funding information

Ministerio de Universidades (Spain), Grant/Award Number: FPU20/07083

Abstract

Plants provide a wide array of compounds that can be explored for potential anticancer properties. Siphonochilone, a furanoterpene that represents one of the main components of the African plant *Siphonochilus aethiopicus*, shows numerous health benefits. However, to date, its antiproliferative properties have not been tested. The aim of this study was to analyze the cytotoxic effects of siphonochilone on a panel of cancer cell lines and its underlying mechanism of action. Our results demonstrated that siphonochilone exhibited significant cytotoxic effects on pancreatic, breast, lung, colon, and liver cancer cell lines showing a IC_{50} ranging from 22 to 124 μM at 72 h of treatment and highlighting its cytotoxic effect against MCF7 and PANC1 breast and pancreas cancer cell lines (22.03 and 39.03 μM , respectively). Cell death in these tumor lines was mediated by apoptosis by the mitochondrial pathway, as evidenced by siphonochilone-induced depolarization of the mitochondrial membrane potential. In addition, siphonochilone treatment involves the generation of reactive oxygen species that may contribute to apoptosis induction. In this work, we described for the first time the cytotoxic properties of siphonochilone and provided data about the molecular processes of cell death. Although future studies will be necessary, our results support the interest in this molecule in relation to their clinical application in cancer, and especially in breast and pancreatic cancer.

KEYWORDS

African ginger, apoptosis, cytotoxic, reactive oxygen species, siphonochilone

1 | INTRODUCTION

Siphonochilus aethiopicus is a member of the family Zingiberaceae commonly known as African ginger or wild ginger. This plant is native of the western and southern tropical Africa. It is used for treating a variety of respiratory ailments¹ and plays significant roles in general well-being maintenance and poverty alleviation through sales of plant

materials for income generation and sustainable livelihoods.² The roots and rhizomes, with similar essential oil composition, have been reported to have potent medicinal properties, as anti-inflammatory, anti-bacterial, and anti-fungal activities, and are known to be used as a spice to flavor food and in traditional herbal medicine for treating fevers, colds, flu, sinusitis, coughs, headache, asthma, malaria, hysteria, candidiasis, epilepsy, and menstrual cramps.³⁻⁵ Consequently, African

This is an open access article under the terms of the [Creative Commons Attribution](https://creativecommons.org/licenses/by/4.0/) License, which permits use, distribution and reproduction in any medium, provided the original work is properly cited.

© 2024 The Authors. *Environmental Toxicology* published by Wiley Periodicals LLC.

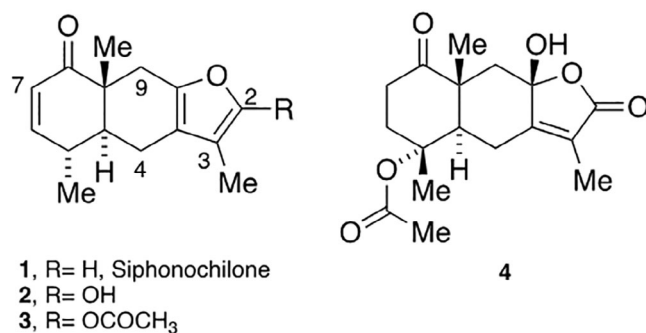


FIGURE 1 Chemical structure of siphonochilones.

ginger is listed in the African Herbal Pharmacopoeia as one of the most important medicinal plants in sub-Saharan Africa,¹ and it is among the eight most traded and the most expensive plant species per kilogram at informal markets in some regions of Limpopo Province in South Africa.⁶

A chemotaxonomic survey of *S. aethiopicus* invariably yielded substantial quantities of an essential oil, with a low content of monoterpenoids, but with substantial amounts (up to 0.2% wet weight) of a major constituent, siphonochilone (1), isolated for the first time in 2002, accompanied by a minor compound, 2-hydroxysiphonochilone (2),⁷ whereas compound 3 has been prepared by acetylation (Ac₂O/Py) of siphonochilone. To date only one more furanoterpenoid from eudesmane family of sesquiterpenoids have been isolated from *S. aethiopicus*, being characterized as 4.⁸ Chemical structures of these compounds are shown in Figure 1.

On the other hand, there is intense research in the discovery of new natural molecules with cytotoxic capacity,⁹ their mechanisms of action¹⁰ and their use as adjuvant therapy.¹¹ In fact, anticancer drugs such as irinotecan, paclitaxel, vincristine, and etoposide have been developed from natural products.¹² In this context, terpenoids, a wide variety of natural products of diverse etiology, have been tested in clinical trials due their antiproliferative properties and even approved as cytotoxic agents.¹³ Within terpenes, the furanoterpenes have been isolated from many different natural resources (i.e., bacteria, algae, corals, marine sponges) and in some cases have been linked to significant cytotoxic capacity. In fact, two metabolites of the furanoterpene C22 from the sponge *Ircinia* sp. (15-acetylcycloformonin B and 10-acetylcycloformonin B) showed significant cytotoxic activity against the K562 (human chronic myelogenous leukemia), DLD-1 (human colon adenocarcinoma), HepG2 and Hep3B (human liver carcinoma) cancer cell lines¹⁴ and furanoterpenes derived from the marine sponge *Gelliodes* sp. showed cytotoxic activity against HeLa (human epidermoid cervical carcinoma), MCF-7 (human breast adenocarcinoma), and A549 (human lung carcinoma) cancer cell lines.¹⁵ Recently, a furanoterpene of *Spongia* sp. from Red Sea demonstrated anti-inflammatory activity and cytotoxicity toward three cancer cell lines including P388 (murine leukemia), HuCCT (human bile duct carcinoma) and DLD-1.¹⁶ Given the rising number of

cancer-related deaths and the failure in conventional treatments, there is an urgent need to develop new therapeutic strategies against this pathology.¹⁷ The demonstrated activity of the furanoterpenes may drive future research on these natural products against some type of cancer.

The aim of this study was to determine the cytotoxic activity of siphonochilone, a furanoterpene from *S. aethiopicus*, using a set of tumor cell lines representative of five tumor types including breast, pancreatic, lung, colon, and liver cancers. We also evaluated the activity of this molecule against a non-tumor cell line. The cytotoxic effect was determined by proliferation and colony formation assays. In addition, the mechanism of action was studied by cell cycle, apoptosis, mitochondrial membrane depolarization, and intracellular ROS accumulation assays in MCF7 and PANC1 cell lines. Taken together, these experiments have provided an insight into the biological activity of siphonochilone and its mechanisms of action on tumor cells, suggesting a new strategy for cancer therapy that will require future trials.

2 | MATERIAL AND METHODS

2.1 | General techniques

The chemical identity of siphonochilone was confirmed by electrospray ionization mass spectrometry (HPLC-ESI-MS; Orbitrap Q-Exactive, Thermo Scientific S.L, Bremen, Germany), and by nuclear magnetic resonance (NMR; Avance III 500 MHz, Bruker, Switzerland). For NMR analyses, the ¹H spectra were recorded at 500 MHz and the ¹³C spectra at 125 MHz, and compound was dissolved in deuterated dimethyl sulfoxide (DMSO-*d*₆), with residual solvent peaks at δ_H = 2.50 (DMSO) ppm for ¹H and δ_C = 39.5 (DMSO) ppm for ¹³C.

2.2 | Plant material

Rhizomes of *S. aethiopicus* were obtained locally from nursery plants grown as ornamentals, sliced, and air-dried. Since *S. aethiopicus* has such a unique and distinctive morphology⁵ and organoleptic characteristics no voucher specimen was collected.

2.3 | Extraction and isolation

Dry crushed rhizome (*S. aethiopicus*, 500 g) was extracted with methanol (2.5 L) at room temperature for 3 days under slow shaking. After this period, the mixture was filtered off and the methanolic solution was concentrated to dryness under vacuum to obtain a syrup (45 g). This syrup was flash chromatographed on silica gel eluting with a mixture of ether:EtOAc (8:2). One fraction was collected (R_f = 0.6, 3.5 g) and identified as siphonochilone (1).

2.4 | Cell culture

Human cancer cell lines A549 (lung), MCF7 and SKBR3 (breast), Mia-PaCa2 and PANC1 (pancreas), T84 and HCT-116 (colon), HepG2 (liver), murine cancer cell lines E0771 (breast) and Panc2 (pancreas), and murine non-tumoral cell line RAW264.7 (macrophage) were grown in Dulbecco's-Modified Eagle's Medium (DMEM)-high glucose (Sigma-Aldrich). T47D human cancer cell line was grown in RPMI 1640 medium (Sigma-Aldrich). Both culture mediums were supplemented with 10% of fetal bovine serum (FBS) (Gibco) and 1% of penicillin/streptomycin (Sigma-Aldrich). In addition, MCF10A breast non-tumoral cell line was grown in DMEM/nutrient mixture F-12 Ham (Sigma-Aldrich) supplemented with 5% horse serum (HS) (Sigma-Aldrich), 0.02 µg/mL epithelial growth factor (EGF) (Sigma-Aldrich), 0.5 µg/mL hydrocortisone (Sigma-Aldrich), 100 ng/mL cholera toxin (Sigma-Aldrich), 10 µg/mL insulin-transferrin-selenium (ITS) (Thermo Fisher Scientific) and 1% of penicillin/streptomycin (Sigma-Aldrich). Cells were maintained at 37°C and 5% CO₂ humidified atmosphere in a monolayer culture.

2.5 | Proliferation assay

Cell lines were seeded in 48-well plates at a density of 2.5×10^3 cells/well for MCF7 and Panc2, 4×10^3 cells/well for E0771, 5×10^3 cells/well for A549 and T84, 8×10^3 cells/well for PANC1, MiaPaCa2 and HCT-116, 10^4 cells/well for MCF10A and RAW264.7, 1.4×10^4 cells/well for T47D, and 5×10^4 cells/well for HepG2. SKBR3 was seeded in 96-well plates at a density of 1.5×10^4 cells/well. After 24 h cells were incubated with increasing concentration (1–250 µM) of siphonochilone for 72 h. Then, adherent cells were fixed with 10% cold trichloroacetic acid (TCA) (Sigma-Aldrich) for 20 min at 4°C. After that, staining with Sulforhodamine B (SRB) (Sigma-Aldrich) (0.08%) diluted in 1% acetic acid glacial (PanReac AppliChem) was performed 20 min at room temperature. The dye was solubilized using Trizma® (10 mM, pH 10.5) (Sigma-Aldrich). Finally, the optical density (OD) was measured at 492 nm using 800™ TS Absorbance Reader (BioTek). Viability assay of RAW264.7 cell line was performed using MTT (3-(4,5-dimethylthiazol-2-yl)-2,5-diphenyltetrazolium bromide) (Sigma-Aldrich) proliferation assay. Briefly, 10% of MTT was added to each well and incubated for 4 h in culture conditions. After this time, 600 µL of dimethylsulfoxide (DMSO) (Sigma-Aldrich) was added per well to dissolve formazan crystal. Finally, the OD was measured at 570 nm using 800™ TS Absorbance Reader (BioTek). Cell viability (%) was calculated as follows:

$$\% \text{Proliferation} = \frac{\text{OD sample} - \text{blank}}{\text{OD negative control} - \text{blank}} \times 100.$$

Additionally, the selectivity index (SI) was used to determine the degree of siphonochilone selectivity toward tumor cell lines compared with non-tumor cells. This index was calculated following:

$$SI = \frac{IC_{50}^{\text{Non-Tumor cells}}}{IC_{50}^{\text{Tumor cells}}}.$$

The importance of this value resides in the fact that the higher the SI value, the greater the selectivity towards tumor cells compared with non-tumor cells. A compound with SI > 2 indicate that are active as anticancer drug and show selectivity.^{18–20}

2.6 | CFSE cell division assay

Cells were trypsinized and stained with 1 µM 5(6)-carboxyfluorescein diacetate succinimidyl ester (CFSE) (Abcam) in PBS at 37°C in the dark for 20 min, after which CFSE excess was removed. Stained cells were then seeded in 6-well plates at a density of 3×10^4 cells/well for MCF7, 9×10^4 cells/well for PANC1 and 1.5×10^5 cells/well for RAW264.7 and MCF10A. Cells were incubated for 1 day allowing adhesion and that time was set as 0 h. MCF7 and PANC1 cell lines were treated with 22 and 39 µM of siphonochilone, respectively, corresponding to its IC₅₀ and non-tumoral cell lines RAW264.7 and MCF10A were treated with 22 and 39 µM, and their IC₅₀ of siphonochilone, 115 µM for RAW264.7 and 82 µM for MCF10A. Cells were collected at 0, 24, 48, and 72 h of treatment and fixed with 4% PFA in PBS at room temperature for 1 h. After that, cells were resuspended in PBS and stored at 4°C until being analyzed in BD FACSCanto II flow cytometer (BD BioSciences). Fold change of CFSE was calculated for each time as follows:

$$\text{Fold change (CFSE)} = \frac{\text{CFSE MFI siphonochilone-treated cells}}{\text{CFSE MFI non-treated cells}},$$

where MFI is the median fluorescence intensity of CFSE. Therefore, low values in the fold change of CFSE (close to 1) indicate a greater effect of the studied compound on cell division.

2.7 | Clonogenic assay

A clonogenic assay was carried out in the selected MCF7 and PANC1 cell lines which were pretreated with 50 and 75 µM of siphonochilone for 72 h. Elapsed this time, the reduction of colony number was assessed by seeding pretreated and non-treated MCF7 (10^2 cells/well) and PANC1 (6×10^2 cells/well) cell lines in 12-well plates. After 24 h, MCF7 non-treated cells were treated with 10 and 20 µM of siphonochilone and PANC1 with 10 and 30 µM of siphonochilone. MCF7 and PANC1 were incubated (7 and 10 days, respectively) at 37°C in fully humidified atmosphere and 5% CO₂. Then, colonies were fixed with cold TCA (Sigma-Aldrich) 10% for 20 min at 4°C and stained for 20 min at room temperature with SRB (Sigma-Aldrich) (0.08%) diluted in 1% acetic acid glacial (PanReac AppliChem), photos were taken, and colonies were counted through an ImageJ software. The experimental conditions of the assays performed are summarized in Table S1.

2.8 | Cell cycle analysis

Cell lines were seeded in 6-well plates at a density of 1.5×10^5 cells/well for MCF7 and 3×10^5 cells/well for PANC1. Both MCF7 and PANC1 cell lines were treated with 100 and 120 μM of siphonochilone, respectively, during 12 and 24 h. Following treatment, the medium was collected, and cells were harvested and centrifuged at 3500 rpm for 3 min. Pellet was resuspended and fixed by adding 900 μL of 70% cold EtOH and placed on ice for 10 min. After fixation, cells were washed with PBS and DNA extraction solution (Na_2HPO_4 0.2 M diluted in 0.1 M acetic acid, pH 7.8) was added and incubated at room temperature for 10 min. This solution was subsequently removed by centrifugation (1500 rpm, 3 min) and pellets were incubated with propidium iodide (PI)/RNAse solution (ImmunoStep) at 37°C for 15 min in the dark. Finally, cells were washed, and the results were acquired using the BD FACSCanto II flow cytometer (BD BioSciences).

2.9 | Apoptosis and mitochondrial membrane potential analysis

The accumulation of cationic cyanine dye in response to membrane potential was studied in association with apoptosis. For this purpose, MCF7 and PANC1 cell lines were seeded in 6-well plates at a density of 1.5×10^5 and 3×10^5 cells/well, respectively. After 24 h, MCF7 and PANC1 cell lines were treated with 100 and 120 μM of siphonochilone, respectively, for 12 and 24 h. Then, assay was performed following the manufacturer's instructions. Briefly, cells were trypsinized, washed with PBS, centrifuged at 3500 rpm for 5 min and pellet was resuspended in PBS and incubated with DiIC1 (ImmunoStep) for 15 min at 37°C. Cells were washed twice with PBS and pellet was resuspended in 1X Annexin-binding buffer and incubated with Annexin V-FITC (ImmunoStep) and PI (ImmunoStep) for 15 min at room temperature in the dark. Finally, cells were analysed in BD FACSCanto II flow cytometer (BD BioSciences). Early apoptosis was determined as the Annexin V+/PI- cell population and late apoptosis was determined as Annexin V+/PI+ cell population.

2.10 | NAC combination proliferation assay

The role of oxidative stress in siphonochilone-induced cell cytotoxicity in breast and pancreatic cancer cells was examined by the addition of the antioxidant N-acetyl-L-cysteine (NAC) (Sigma-Aldrich). Pretreatment of cells with ROS scavenger such as NAC can effectively inhibit the reactive species-induced cellular response including ROS-mediated cell death. MCF7 and PANC1 cell lines were seeded in 48-well plates at a density of 2.5×10^3 and 8×10^3 cells/well, respectively. After 24 h cells were pretreated with non-toxic NAC concentrations (0.5 and 8 mM for MCF7 and PANC1, respectively) for 2 h. Elapsed this time, different doses of siphonochilone were used to the treatment of MCF7 (20, 50, and 75 μM) and PANC1 (50, 75, and

100 μM) for 72 h. Then SRB proliferation assay was performed as previously described.

2.11 | Intracellular ROS measurement

Intracellular reactive oxygen species (ROS) accumulation in MCF7 and PANC1 cells after treatment with siphonochilone was detected using the 2',7'-dichlorodihydrofluorescein diacetate assay (DCFDA) (Abcam). Cell lines were seeded in 6-well plates at a density of 10^5 cells/well for MCF7 and 1.5×10^5 cells/well for PANC1 and in 96-well plates at a density of 3×10^3 cells/well for MCF7 and 10^4 cells/well for PANC1. Both MCF7 and PANC1 cell lines were treated with 100 μM and 250 μM of siphonochilone, respectively, during 4 and 12 h. After treatment, medium was discarded, and 6-well plates cells were harvested and centrifuged at 3500 rpm for 3 min. In both cases, cells were washed with PBS and stained for 30 min at 37°C with 20 μM DCFDA and PI (1:25) for cytometry and Hoechst (1:1000) for microscopy. The 2',7'-dichlorofluorescein (DCF) probe was visualized using the fluorescence microscopy (Leica) and analyzed using BD FACSCanto II flow cytometer (BD BioSciences).

2.12 | Prediction of potential targets and structural similarity of siphonochilone

Based on the molecular structure of siphonochilone, a structure-activity relationship (SAR) study was performed by exploring its possible molecular targets. SwissTargetPrediction (<http://www.swisstargetprediction.ch/>),²¹ an open-access database for ligand-based target prediction was employed to identify the potential targets of siphonochilone. Transformation of the siphonochilone molecular structure into canonical SMILES was achieved through the PubChem platform (<https://pubchem.ncbi.nlm.nih.gov/>). Subsequently, this canonical SMILES representation was input into the SwissTargetPrediction interface. The screening condition was established by selecting "Homo sapiens" as the designated species and considering probabilities greater than 0. Additionally, SwissSimilarity (<http://www.swissimilarity.ch/>)²² free access tool was employed for the identification of ligands within approved drug molecules exhibiting structural similarity to siphonochilone. The SMILES code was submitted as a query to the SwissSimilarity website, wherein the compound class "Drugs" was selected, and the library "ChEMBL approved drugs" was chosen, employing a combined methods approach.

2.13 | Statistical analysis

Different statistical tests were employed, depending on the type of data under analysis. All statistical analyses and graphical representations were carried out using the Graphad Prism 9 software. To compare two groups, the Student *t*-test was performed. For comparisons involving multiple samples, one-way ANOVA (univariate comparison)

TABLE 1 Determination of IC₅₀ (μM)^a of siphonochilone in different cell lines.

Organ	Cell line	Origin	Disease	Cells/well	Siphonochilone ^a
Breast	MCF7	H	AD	2.5 × 10 ³	22.03 ± 1.79
	T47D	H	C	1.4 × 10 ⁴	30.19 ± 5.59
	SKBR3	H	AD	1.5 × 10 ^{4b}	108.02 ± 37.07
	MCF10A	H	NT	10 ⁴	81.64 ± 29.83
	E0771	M	C	4 × 10 ³	50.42 ± 16.54
Pancreas	PANC1	H	C	8 × 10 ³	39.03 ± 4.12
	MiaPaCa2	H	C	8 × 10 ³	35 ± 14.19
	Panc2	M	AD	2.5 × 10 ³	23.01 ± 12.59
Lung	A549	H	C	5 × 10 ³	41.81 ± 17.52
Colon	T84	H	C	5 × 10 ³	124.57 ± 15.44
	HCT-116	H	C	8 × 10 ³	33.56 ± 4.36
Liver	HepG2	H	C	5 × 10 ⁴	87.83 ± 7.16
Bone marrow	RAW264.7	M	NT	10 ⁴	115.5 ± 48.85

Abbreviations: AD, adenocarcinoma; C, carcinoma; H, human; M, mouse; NT, non-tumoral.

^aHalf-maximal inhibitory concentration (IC₅₀) values calculated from dose-response curves as the concentration of compound that inhibits cell survival by 50% compared with control. They are expressed as means ± SD of triplicate samples each.

^bCell number in 96-well plates, the rest of the cell lines were seeded in 48-well plates.

TABLE 2 The selectivity index (IC₅₀ non-tumor cell line/IC₅₀ tumor cell line) of siphonochilone for each of the cell lines used in this study.

	MCF7	T47D	SKBR3	E0771	PANC1	MiaPaCa2	Panc2	A549	T84	HCT116	HepG2
MCF10A	3.71	2.7	0.76	1.62	2.09	2.33	3.54	1.95	0.66	2.43	0.93
RAW264.7	5.24	3.83	1.07	2.29	2.96	3.3	5.02	2.76	0.93	3.44	1.32

and two-way ANOVA (comparison of two variables) were employed. For cytotoxicity analysis, a non-linear regression was conducted to calculate logEC₅₀. Statistical significance was determined for differences with a *p*-value less than .05.

3 | RESULTS

3.1 | Siphonochilone shows cytotoxicity against several tumor cell lines

Cell viability and proliferation assays were used to evaluate the impact of siphonochilone in tumoral cells as a possible anticancer treatment.²³ Cytotoxic effect of siphonochilone was evaluated in a panel of 11 tumor cell lines of different origins (breast, pancreas, lung, colon, and liver) and specie (human and mouse) after 72 h of drug exposure siphonochilone showed a half maximal inhibitory concentration (IC₅₀) range between 22 and 124 μM in the tested cell lines (Table 1). The most resistant cell line was the T84 human colon cancer cell line (IC₅₀ = 124.57 μM). By contrast, MCF7 human breast cancer cell was the cell line more sensible to siphonochilone showing the lowest IC₅₀ (22.03 μM). The non-tumoral breast cell line (MCF10A) and macrophage cell line (RAW264.7) were also analyzed which showed a significantly higher IC₅₀ (81.64 and 115.5 μM, respectively) than the majority of tumor cell line. Furthermore, among the tested murine cell

lines, E0771 breast cancer cell line showed higher IC₅₀ (50.42 μM) than Panc2 pancreatic cancer cell line (23.01 μM).

In addition, the therapeutic effectiveness of siphonochilone as an anticancer agent was evaluated using the SI (Table 2). Eight of the eleven tumor cell lines tested showed a SI>2 in at least one of the two non-tumor cell lines studied. The SI>2 of the cell lines ranged from 2.09 to 3.71 compared with MCF10A and from 2.29 to 5.24 compared with RAW264.7. However, SKBR3, T84, and HepG2 cell lines showed SI values lower than 2 for both non-tumor cell lines. Their SI values ranged from 0.66 to 0.93 compared with MCF10A and from 0.93 to 1.32 compared with RAW264.7.

3.2 | Siphonochilone induces inhibition of cell division

CFSE assay was used to determine the implications of siphonochilone in cell division. As shown in Figure 2A, fluorescence intensity of CFSE-labeled cells decreases by half at each cell division. MCF7 and PANC1 tumor cell lines exposed to siphonochilone IC₅₀, exhibited a fold change in fluorescence intensity of 2.37 and 2.80 times higher, respectively, than their respective controls at 72 h (Figure 2B,C). A similar trend of reduced cell division dose-dependent was also observed in the RAW264.7 and MCF10A non-tumor cell lines (Figure 2D,E). It should highlight that the MCF10A human non-tumor

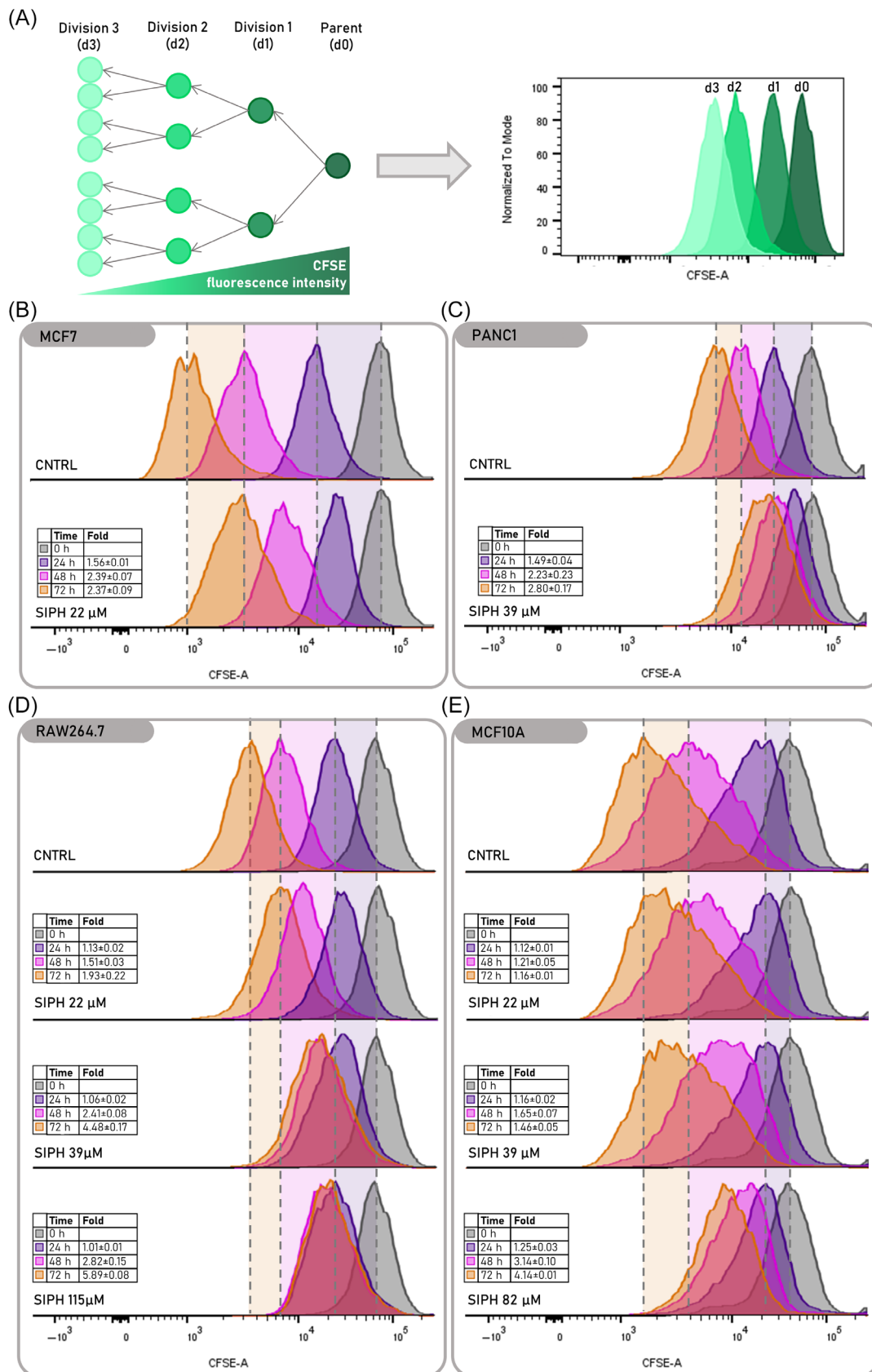


FIGURE 2 Reduction in cell division rate after siphonochilone treatment. The fluorescent signal of CFSE decreases by 50% with each cellular division, and fluorescence detection is achieved through flow cytometry (A). Graphical representation of CFSE fluorescence intensity in siphonochilone treated and non-treated MCF7 (B), PANC1 (C), RAW264.7, (D) and MCF10A (E) cells at different treatment times (0, 24, 48, and 72 h). Fold indicates fold change (CFSE)=(CFSE MFI siphonochilone-treated cells)/(CFSE MFI non-treated cells) for each time, where MFI is the median fluorescence intensity.

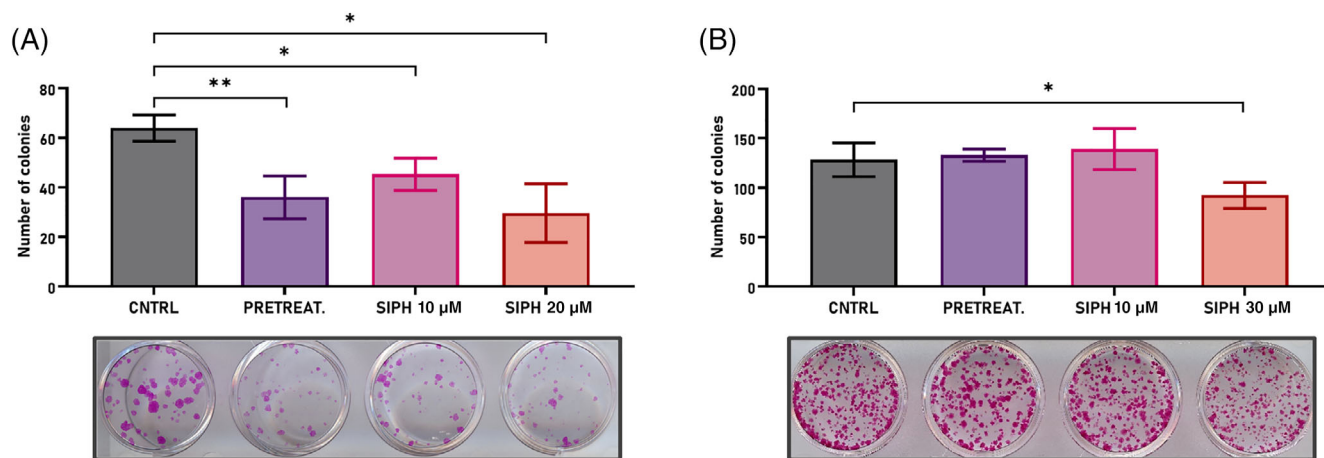


FIGURE 3 Clonogenic assay after human tumor cell lines exposure to siphonochilone. Colony growth analysis of MCF7 (A) and PANC1 (B) after siphonochilone treatment. Data represent the mean value \pm SD of three replicates. * $p < .05$ and ** $p < .01$.

cell line exposed to 22 and 39 μM of siphonochilone only increased the fold change of CFSE fluorescence intensity in 1.16 and 1.46 times, respectively. These values were lower than those found in tumor cell lines at the same siphonochilone concentrations. Therefore, a significant increase of CFSE labeling was evident in siphonochilone-treated cells compared with their respective untreated control, indicating a reduction in cell division.

3.3 | Siphonochilone reduces cell colony formation capacity in breast and pancreatic tumor cells

MCF7 and PANC1 cell lines characterized by a high proliferation rate and a low siphonochilone IC_{50} were selected to determine the long-term effect of the furanoterpenoid using a clonogenic assay. Colony formation assays are based on the principle that normal cells need contact with the surrounding cells and the extracellular matrix to proliferate. In contrast, transformed or malignant cells can proliferate independently of their surrounding environment. Consequently, the most aggressive cells will develop colonies, and the quantification of these colonies provides a measure of the malignant potential.²³ As shown in Figure 3A, colony formation in MCF7 was significantly decreased in pretreated cells and cells exposed to 10 and 20 μM of siphonochilone. On the other hand, PANC1 cells only showed a significant decrease in colony-forming capacity when the highest siphonochilone dose (30 μM) was used (Figure 3B).

3.4 | Siphonochilone modulates cell cycle progression

Detecting alterations in the cell cycle's progression is a crucial aspect of drug development. This is essential because it can provide valuable data that helps to elucidate the mechanism of action of the drug.²⁴ Our results showed that both MCF7 and PANC1 cell lines were arrested by siphonochilone at the G2/M cell cycle phase. An increase

in cells in G2/M phase after 12 and 48 h of siphonochilone treatment (16% and 8% at respectively) was observed (Figure 4A). Similar results were observed in PANC1 although G2/M arrest was statistically significant only after 12 h (12% of increase) of siphonochilone treatment (Figure 4B). In addition, a progressive time-dependent increase of cell percentage in SubG1 phase was observed in MCF7 cells after siphonochilone treatment (Figure 4C). These differences were less marked in PANC1 cell line (Figure 4D).

3.5 | Apoptosis and mitochondrial membrane potential

Investigating mitochondrial function, a pivotal indicator of cell health, involves evaluating alterations in mitochondrial membrane potential. Therefore, disruption of mitochondrial function is an effect caused by some antitumor drugs that has gained attention in recent years.²⁵ Mitochondrial membrane depolarization analysis of MCF7 cell line did not show any significant change in mitochondrial depolarization (Figure 5A,B). By contrast, siphonochilone treatment induced mitochondrial depolarization in PANC1 cell line at 12 and 48 h in both IP+ and IP- labeled cells (Figure 5A,C). Concretely, after siphonochilone exposure, the increase in the percentage of cells with altered mitochondrial membrane potential (DiIC-) reached a 46% and 41% at 12 and 24 h, respectively. Furthermore, as shown in Figure 5D, a strong cytotoxic effect was observed in PANC1 after siphonochilone treatment (12 and 24 h) causing cell death by both early and late apoptosis (ranging from 22% to 27%) (Figure 5F). By contrast, there was not a significant annexin V increase in MCF7 cells (Figure 5E).

3.6 | NAC pretreatment reduces cytotoxic effect of siphonochilone

ROS are considered as typical byproducts of numerous cellular processes. Nevertheless, elevated ROS levels can cause damage to

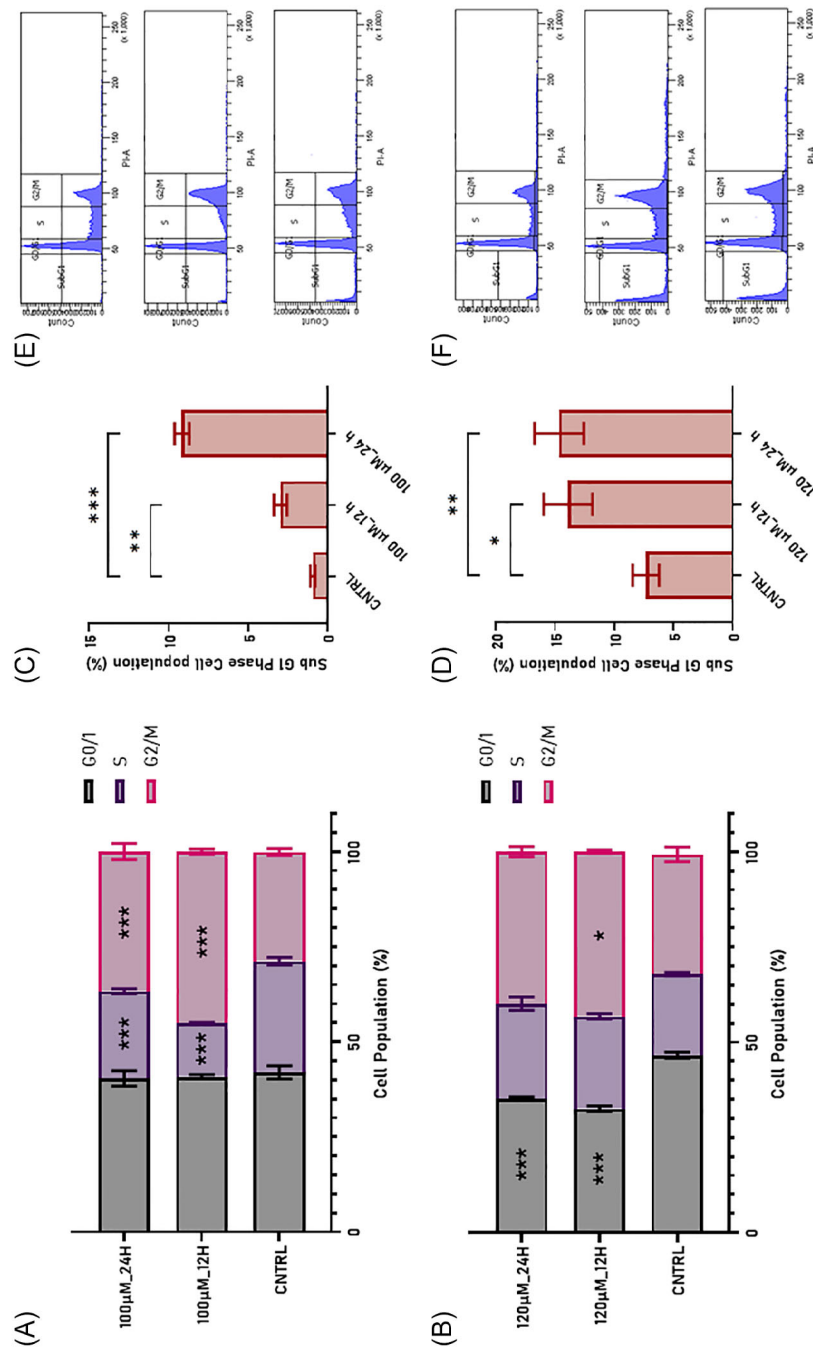


FIGURE 4 Flow cytometry cell cycle analysis of tumor cells after siphonochilone treatment. Graphical representation of G0/1, S and G2/M phases of cell cycle after treatment with siphonochilone at 12 and 24 h in MCF7 (A) and PANC1 (B) cell lines. Modulation Sub G1 cell cycle phase by siphonochilone in MCF7 (C) and PANC1 (D). Representative images of cell cycle analysis in MCF7 (E) and PANC1 (F) from top to bottom: control and 12 h and 24 h treatment with siphonochilone. Data represent the mean value \pm SD of three replicates. * $p < .05$, ** $p < .01$ and *** $p < .001$ versus control group.

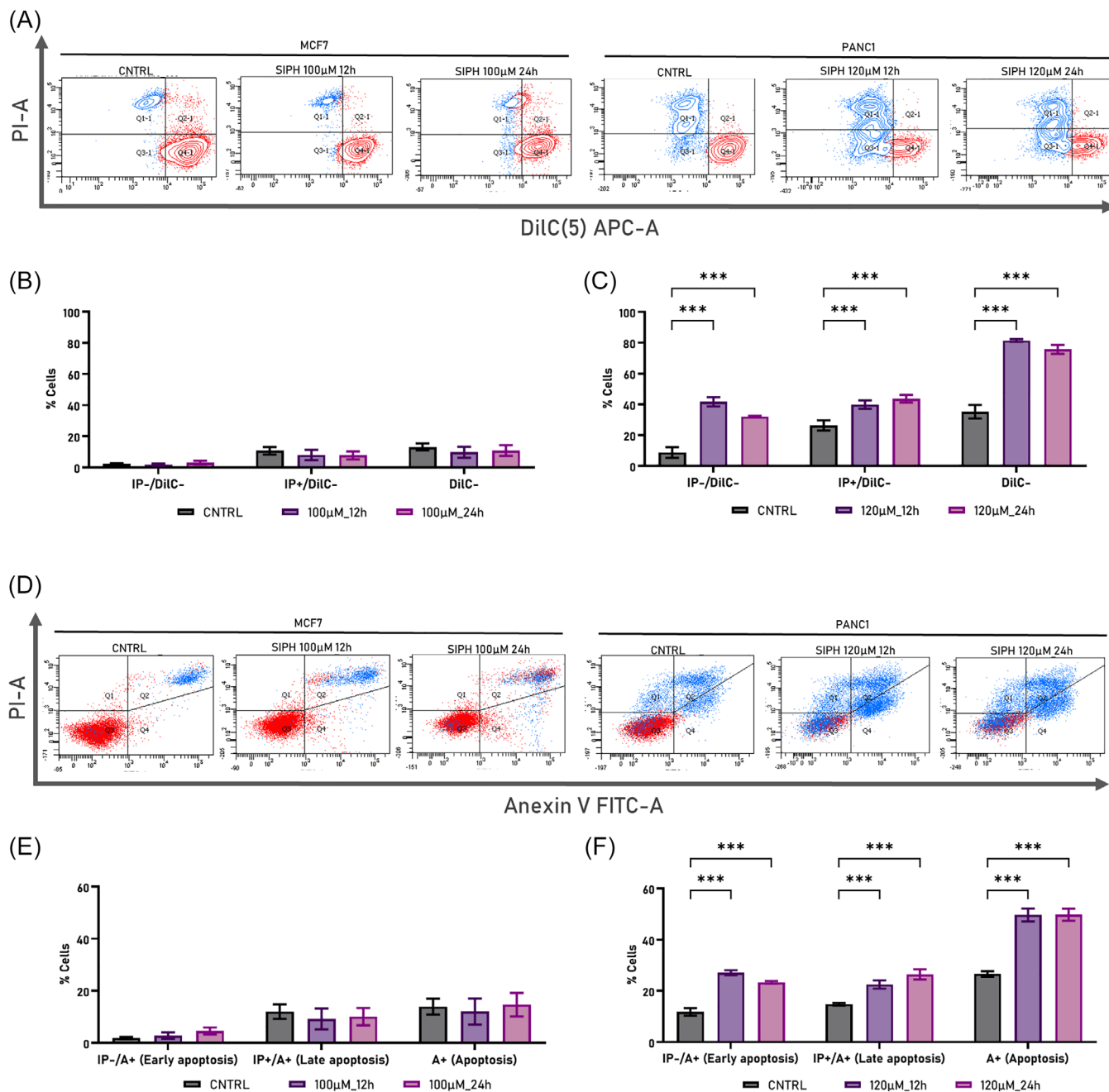


FIGURE 5 Proapoptotic activity and mitochondrial membrane depolarization in response to siphonochilone treatment in MCF7 and PANC1 cell lines. (A) Representative images of membrane potential assay using DiIC and PI in MCF7 and PANC1. Graphical representation of mitochondrial membrane depolarization after treatment with siphonochilone at 12 and 24 h in MCF7 (B) and PANC1 (C) cell lines. (D) Representative images of apoptosis analysis using Annexin V and PI in MCF7 and PANC1. Graphical representation of apoptotic cells after treatment with siphonochilone at 12 and 24 h in MCF7 (E) and PANC1 (F) cell lines. Data represent the mean value ± SD of three replicates. *** $p < .001$ versus control group.

nucleic acids, proteins, lipids, organelles, and membranes, leading to cell death.²⁶ Then, ROS play a crucial role in the regulation of cell death and survival in cancer cells. In this context, we used NAC to determine the involvement of ROS in cell death mechanism of siphonochilone. NAC-pretreated MCF7 and PANC1 cells at 0.5 and 8 mM, respectively, exhibited higher viability than those without

NAC pretreatment. The most protective effects of NAC were observed at the highest doses of siphonochilone in both MCF7 (Figure 6A) and PANC1 (Figure 6B) cells. For instance, the use of NAC reduced cell death by $25.1\% \pm 2.4\%$ in MCF7 and $48.7\% \pm 6.3\%$ in PANC1, when cells were exposed to 75 µM of siphonochilone.

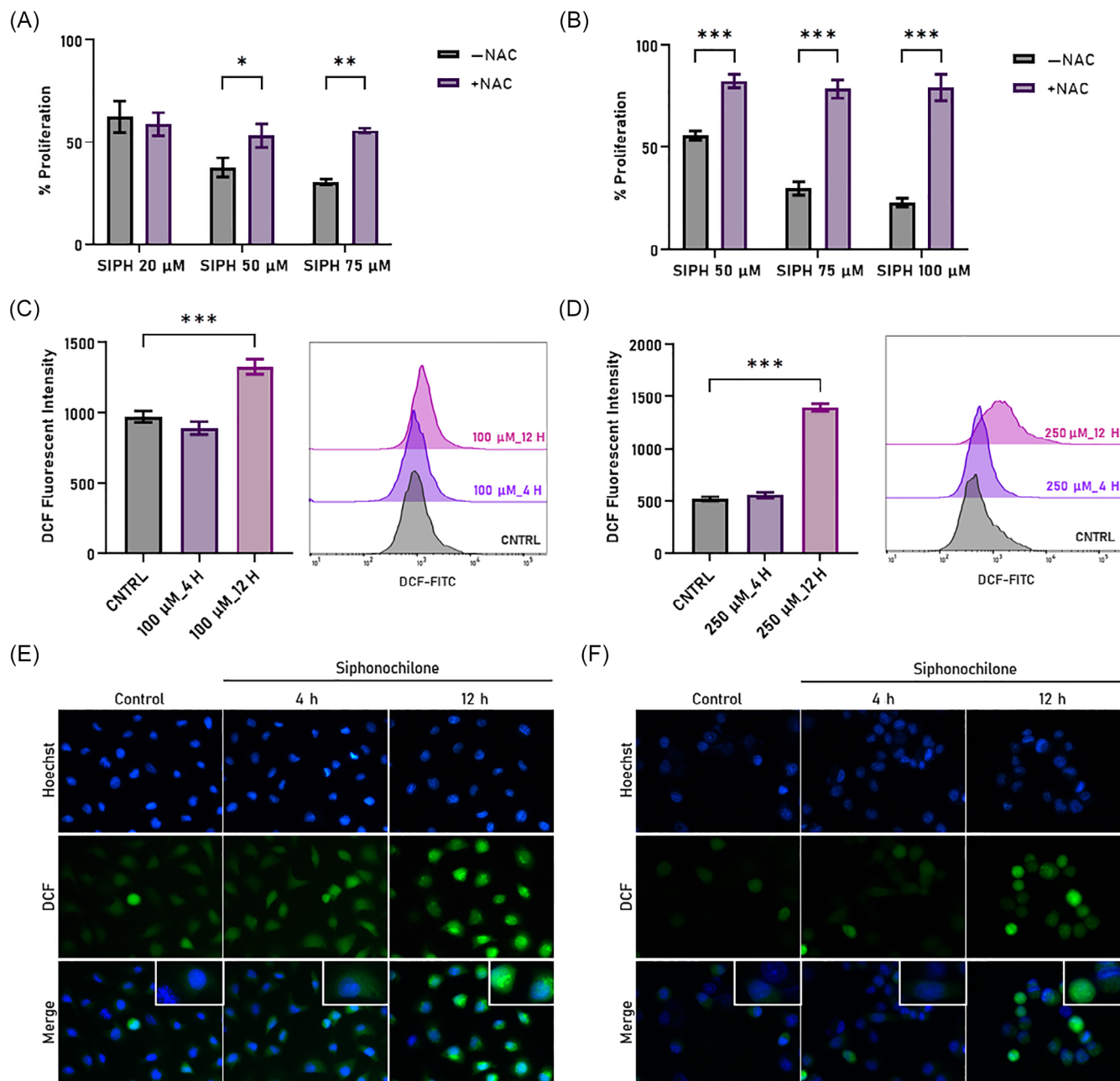


FIGURE 6 Reactive oxygen species (ROS) generation by siphonochilone in MCF7 and PANC1 tumor cell lines. Percentage of cell proliferation (% proliferation) in MCF7 (A) and PANC1 (B) cells after siphonochilone treatment with and without NAC pretreatment. Flow cytometry determination of intracellular ROS in MCF7 (C) and PANC1 (D) cells. Data represent the mean value \pm SD of three replicates. * $p < .05$, ** $p < .01$, and *** $p < .001$ versus control group. Representative fluorescent microscopy images showing intracellular ROS (green) and Hoechst (blue) staining in MCF7 (E) and PANC1 (F) cells. Magnification 40X.

3.7 | Intracellular ROS levels increase after siphonochilone treatment

To assess intracellular ROS levels in cells treated with siphonochilone for 4 and 12 h, cells were loaded with a ROS probe (DCFDA) and DCF fluorescent intensity was measured by flow cytometry. Our results showed that ROS levels significantly increased after

12 h of siphonochilone exposure in both MCF7 (Figure 6C) and PANC1 (Figure 5D) (37% and 168%, respectively) compared with control. However, to a shorter exposure time (4 h), siphonochilone did not induce differences in ROS formation in any of cell lines compared with the control. ROS generation was further confirmed by fluorescence microscopy in MCF7 (Figure 6E) and PANC1 (Figure 6F).

3.8 | Potential protein target and similarity search

SwissTargetPrediction analysis resulted in targets on three different classes: 56% family A G protein-coupled receptor (Muscarinic acetylcholine receptor M1–M5), 33% electrochemical transporter (norepinephrine, serotonin, and dopamine transporter) and 11% membrane receptor (sigma opioid receptor), but with a low probability in all of them (0.05) (Figure S1A). Also, SwissSimilarity was used to compare the structure of siphonochilone with approved drugs and thus to compare their potential biological activity, as well as to predict the possible application. A total of 30 small molecules were found with a similarity score greater than 0 (Figure S1B). Highest similarity score with a value of 0.394 was found between siphonochilone and Trioxsalen, a drug used for the treatment of psoriasis. Among these 30 molecules, three of them are related to the treatment of neoplasms: methoxsalen, erlosamide, and tolbutamide (Table S2).

4 | DISCUSSION

In the present study we reported the cytotoxic effect of siphonochilone against a panel of human and mouse tumor cell lines and the action mechanism by which it exerts its antiproliferative effect. To our knowledge, it is the first time that the cytotoxic effect of siphonochilone against tumor cell lines has been analyzed. Our findings revealed that siphonochilone displayed significant cytotoxic effects on cancer cell lines from different tissue origins including those derived from the pancreas, breast, lung, colon, and liver. Interestingly, the IC_{50} value of MCF-10A breast non-tumor cell line (81.64 μ M) was higher than the rest of breast cancer cell lines, with the exception of the SKBR3. Additionally, the IC_{50} value of RAW264.7 murine non-tumoral cell line was only exceeded by T84 metastatic colorectal cancer cell line (115.5 versus 124.57 μ M). This result suggests a potential selectivity of the siphonochilone toward tumor cells. Regarding the SI, both cell lines mainly tested in this study showed a $SI > 2$. Specifically, MCF7 showed a SI of 3.71 and 5.24 compared with MCF10A and RAW264.7, respectively, and the PANC1 cell line showed a SI of 2.09 and 2.96 compared with MCF10A and RAW264.7, respectively. Low selectivity of the antitumor drugs currently in use is one of the main limitations in cancer therapy.²⁷ Nevertheless, nowadays drugs with low selectivity rates are being used for the treatment of different types of cancer. For instance, some authors have reported that the SI values in MCF7 for doxorubicin is 0.57 and for cisplatin 0.58,²⁸ and for paclitaxel 0.94.²⁹ Although, new studies will be necessary to determine the selectivity of siphonochilone and its mechanisms of action, our results suggest that it could be a good candidate for therapeutic development. For future research, a possible approach to increase the SI toward cancer cells could be the encapsulation of siphonochilone in nano-systems to promote its controlled release at the target site. In fact, association of natural compounds in drug delivery methods may increase stability, effectiveness and bioavailability, and reduce side effects.²⁷ For instance, Ren et al. developed a nanocarrier for efficient delivery of doxorubicin to cancer cells, increasing the selectivity

of the drug.³⁰ Furthermore, Jiang et al. found that curcumin, a natural product derived from a member of the Zingiberaceae family, loaded in nanoparticles enhances selectivity toward MCF7 and MDA-MB-231 tumor cells compared with RAW264.7 and CHO non-tumor cells.³¹ Few studies about the cytotoxic activity of furanoterpenoids from *S. aethiopicus* have been described. Igoli et al. reported that sesquiterpenes epi-curzerenone and furanodienone, isolated from *S. aethiopicus*, did not exhibit cytotoxicity activity (even at 100 μ g/mL) whereas the 8 (17),12E-labdadiene-15,16-dial displayed a significant cytotoxicity against SH-SY5Y (neuroblastoma), L929 (murine fibrosarcoma) and Jurkat (leukaemia) cell lines and a moderate effect on Hs 27 (normal foreskin) cell line.³² In addition, Lategan et al. analyzed the cytotoxic effect of three furanoterpenoids isolated from *S. aethiopicus* against the CHO, a Chinese hamster ovary cell line used to assess the toxicity of drugs, showing a higher IC_{50} value than those obtained with the ethyl acetate extract of the plant.³³

CFSE analysis showed that siphonochilone decreased cell division in MCF7, PANC1, RAW264.7, and MCF10A cell lines. However, there are some points that need to be highlighted. When examining the effect of siphonochilone on cell division at equal doses among the tumor cell lines and MCF10A, the reduction in division was more evident in the tumor cell lines. Nevertheless, when comparing at equal doses with RAW264.7, division in MCF7 was lower, but the same did not occur at the IC_{50} dose of PANC1. Thus, a generalized differential effect on cell division between tumor and non-tumor cell lines remains unclear. The reduction in cell division rate of tumor cells was consistent with alteration in the cell cycle. Our results indicated that siphonochilone caused cell cycle arrest in G2/M phase along with an increase in the number of cells in the Sub G1 phase, an effect dependent on the time of exposure to siphonochilone in MCF7 and PANC1 cell lines. Few data have been described on the activity of furanoterpenoid molecules in the cell cycle. Li et al. demonstrated that 20–80 mM furanodienone led to a dose-dependent increase in sub G1 phase cell populations when administered in the presence of 17β -estradiol.³⁴ Therefore, compounds similar to the one tested in this study cause a disruption in the progression of the cell cycle.

Concerning cell death mechanisms, following the observed SubG1 increase, an analysis of programmed cell death or apoptosis was conducted. Upon treatment with siphonochilone PANC1 pancreatic cancer cell line displayed an increase in the percentage of apoptotic cells, along with an increase in mitochondrial membrane depolarization. The negative results of MCF7 cells in apoptosis induction could be due to not functional mechanisms of apoptosis present in this cell line that have been related to the lack of the caspase 3 effector.³⁵ On the other hand, only with the use of furanodienone an opening of mitochondrial permeability transition pores (mPTP) has been described in glioma cells³⁶ suggesting mitochondrial damage and supporting our results with the use of siphonochilone. In a similar way, an increase in breast and colorectal cancer cell lines apoptosis after furanodienone treatment has been described.^{37,38} Efficient eradication of cancer cells through programmed cell death, also known as apoptosis, has been a fundamental objective and goal of clinical cancer therapy for years.³⁹

Interestingly, the increased intracellular ROS production in tumor cells by some antitumor drugs is one of the main mechanisms to induce cytotoxicity.^{40,41} ROS are responsible for cell death mechanisms such as apoptosis or autophagy.^{26,42} Therefore, we hypothesized that apoptosis may be triggered by the generation of ROS. Previous studies suggested that the cytotoxic effects of furanoterpenoids, such as furanodienone, could be attributed to ROS production. In fact, Jiang et al. showed that treatment with the antioxidant NAC attenuated the cytotoxic effects mediated by ROS.³⁸ Similar results were obtained with siphonochilone, where combined treatment with the antioxidant NAC reduced the cytotoxicity induced by treatment with siphonochilone alone. These findings suggest the involvement of ROS in the cell death mechanism associated with siphonochilone. Furthermore, our results showed a significant increase in ROS production after 12 h of treatment in both cell lines, PANC1 and MCF7. In fact, some classical cytotoxic drugs used in clinical practice such as cisplatin⁴³ are able to activate this cellular death mechanism. Additionally, it has been demonstrated that natural sesquiterpenes such as alantolactone⁴⁴ can also modulate ROS production, suggesting that siphonochilone might act through ROS to induce its demonstrated cytotoxic activity.

Regarding SAR study, although the three possible families of target proteins (family A G protein-coupled receptor, electrochemical transporter and membrane receptor) have the potential to participate in the tumor process through their functions in cell signaling, substance transport, and survival cell, the virtual screening performed in SwissTargetPrediction could not find any targets with a high binding probability. However, the SwissSimilarity study yielded 30 molecules with a score > 0 structurally similar to siphonochilone. These small molecules with similarity to siphonochilone showed a wide range of action with applications in many different diseases. Among them, those related to the treatment of neoplasms include methoxsalen, erlosamide, and tolbutamide. Erloramide, commonly known as lacosamide, showed a dose-dependent cytotoxic and anti-migratory effects in human glioma cell lines U87MG, SW1483, and T98G, with IC₂₀ of 300, 625 and 1178 μ M, respectively. Lacosamide effects appeared to be mediated by the regulation of miRNAs.⁴⁵ Additionally, SM-88 has been used in a clinical trial combined with methoxsalen, phenytoin, and sirolimus in pretreated metastatic pancreatic ductal adenocarcinoma (mPDAC) (NCT03512756) with encouraging effects on patients' quality of life, disease control, and survival.⁴⁶ The current findings indicate that siphonochilone will require extensive experimental validation to elucidate their molecular targets. However, given its similarity to molecules approved in the clinic for a wide range of diseases, it could have alternative uses to cancer treatment.

Siphonochilone has been isolated from *S. aethiopicus*, commonly known as African ginger. Ginger has been used as a medicinal herb for centuries and provides multiple health benefits. Ginger's clinical applications have undergone extensive examination, leading to a substantial number of clinical trials that examine the improvement of vomiting and nausea, inflammation, metabolic syndromes, digestive function, and markers of colorectal cancer.⁴⁷ Nonetheless, the existing literature does not present clinical trials involving any compounds

derived from the Zingiberaceae family as cytotoxic drugs. However, various studies have revealed the therapeutic potential of ginger and its bioactive components in a tumor context. This potential was evidenced by their cytotoxic effects on tumor cell lines, influence on enzymatic activities, synergy with chemotherapy, plausible interactions with the microbiota, and advancements in utilizing nanoparticles loaded with these bioactive compounds.⁴⁸ [10]-Gingerol, a bioactive compound found in ginger roots, demonstrated a robust cytotoxic effect against triple-negative breast cancer cell lines. This effect was achieved through the mechanism of cell cycle arrest and cell death, mainly mediated by apoptosis induced by mitochondrial outer membrane permeabilization.⁴⁹ These mechanisms are similar to those triggered by siphonochilone, as explored in the current study. Furthermore, *S. aethiopicus* ethanol and diethyl ether extracts caused a decrease in viability, as well as damage to the cell membrane and cell death through apoptosis and necrosis processes.⁵⁰ Taken together, the Zingiberaceae family presents a diverse array of potential health benefits. Siphonochilone is a relatively underexplored compound derived from *S. aethiopicus* that exhibits potential clinical relevance. To further explore its potential, it is imperative to continue investigating its underlying molecular mechanisms and its broad range of physiological effects. Additionally, future *in vivo* experiments will allow us to bring this molecule closer to a potential clinical trial.

Despite the results obtained, our work has certain limitations that could be addressed in the future, such as (i) the study of a greater number of breast and pancreatic cancer cell lines; (ii) the study of other mechanisms of cell death, (iii) the analysis of the combination of siphonochilone with drugs commonly used in the clinic to determine the synergistic effect, and (iv) *in vivo* studies. However, although further study is needed, preliminary results show that siphonochilone is a potential antitumor agent that we should explore.

5 | CONCLUSIONS

We analysed the siphonochilone-induced antitumor effects *in vitro* using a panel of tumor cell lines that included breast, pancreatic, lung, colon, and liver cancer. A further investigation about siphonochilone cell death mechanism was carried out using the MCF7 breast cancer and the PANC1 pancreatic cancer cell lines. Our findings demonstrated that siphonochilone significantly induced G2/M phase arrest and activated cell apoptosis via ROS-dependent mitochondrial pathway. To our knowledge, it is the first time that the cytotoxic effect of siphonochilone against tumor cells has been observed. This research provides valuable insight into the molecular processes underlying siphonochilone-induced cell death, offering potential implications for the clinical development of this new drug as a cancer treatment, and specifically breast and pancreatic cancer.

AUTHOR CONTRIBUTIONS

Alba Ortigosa-Palomo: Investigation; formal analysis; writing. **David Fuentes-Ríos and Francisco Quiñonero:** Investigation; formal analysis. **Raul Ortiz and Consolación Melguizo:** Conceptualization;

Writing—original draft. **Juan M. López-Romero**: Conceptualization; Writing. **Jose Prados**: Conceptualization; Writing—original draft. All authors reviewed the manuscript and provided comments or suggestions. All authors read and approved the final manuscript.

ACKNOWLEDGEMENTS

We thank the FQM397 research group of the University of Malaga. A. Ortigosa-Palomo acknowledges FPU2020 grant (ref. FPU20/07083) from the Ministerio de Universidades (Spain). Funding for open access charge: Universidad de Granada/CBUA.

CONFLICT OF INTEREST STATEMENT

The authors declare no conflict of interest.

DATA AVAILABILITY STATEMENT

The data that support the findings of this study are available from the corresponding author upon reasonable request.

ORCID

Raul Ortiz  <https://orcid.org/0000-0001-8409-5235>

REFERENCES

- van Wyk BE. A broad review of commercially important southern African medicinal plants. *J Ethnopharmacol.* 2008;119:342-355.
- Adebayo SA, Amoo SO, Mokgehele SN, Aremu AO. Ethnomedicinal uses, biological activities, phytochemistry and conservation of African ginger (*Siphonochilus aethiopicus*): A commercially important and endangered medicinal plant. *J Ethnopharmacol.* 2021;266:113459.
- Igoli NP, Al-Tannak NF, Ezenyi IC, Gray AI, Igoli JO. Antiplasmodial activity of a novel diarylheptanoid from *Siphonochilus aethiopicus*. *Nat Prod Res.* 2021;35:5588-5595.
- Viljoen AM, Demirci B, Başer KHC, Van Wyk BE. The essential oil composition of the roots and rhizomes of *Siphonochilus aethiopicus*. *S. Afr. J. Bot.* 2002;68:115-116.
- Van Wyk BE. The potential of South African plants in the development of new medicinal products. *S. Afr. J. Bot.* 2011;77:812-829.
- Moeng ET, Potgieter MJ. The trade of medicinal plants by muthi shops and street vendors in the Limpopo Province, South Africa. *J. Med. Plants Res.* 2011;5:558-564.
- Holzappel CW, Marais W, Wessels PL, Van Wyk BE. Furanoterpenoids from *Siphonochilus aethiopicus*. *Phytochemistry.* 2002;59:405-407.
- Al-Tannak NF, Anyam JV, Igoli NP, Gray AI, Alzharani MA, Igoli JO. A new sesquiterpene from South African wild ginger (*Siphonochilus aethiopicus* (Schweinf) B.L. Burt). *Nat Prod Res.* 2022;36:4943-4948.
- Dehelean CA, Marcovici I, Soica C, et al. Plant-derived anticancer compounds as new perspectives in drug discovery and alternative therapy. *Molecules.* 2021;26:1109.
- Hashem S, Ali TA, Akhtar S, et al. Targeting cancer signaling pathways by natural products: Exploring promising anti-cancer agents. *Biomed. Pharmacother.* 2022;150:113054.
- Lin SR, Chang CH, Hsu CF, et al. Natural compounds as potential adjuvants to cancer therapy: Preclinical evidence. *Br J Pharmacol.* 2020;177:1409-1423.
- Huang M, Lu JJ, Ding J. Natural products in cancer therapy: Past present and future. *Nat Prod Bioprospect.* 2021;11:5-13.
- Kamran S, Sinniah A, Abdulghani MAM, Alshawsh MA. Therapeutic potential of certain terpenoids as anticancer agents: A scoping review. *Cancers.* 2022;14(5):1100.
- Su JH, Tseng SW, Lu MC, Liu LL, Chou Y, Sung PJ. Cytotoxic C 21 and C 22 terpenoid-derived metabolites from the sponge *Ircinia* sp. *J Nat Prod.* 2011;74:2005-2009.
- Ki DW, Kodama T, el-Desoky AH, et al. Chemical constituents of the Vietnamese Marine Sponge *Gelliodes* sp. and their cytotoxic activities. *Chem Biodivers.* 2020;17:e2000303.
- Tai CJ, Huang CY, Ahmed AF, et al. An anti-inflammatory 2,4-cyclized-3,4-secospongian diterpenoid and furanoterpene-related metabolites of a marine sponge *Spongia* sp. From the red sea. *Mar Drugs.* 2021;19:38.
- Brennan P, Davey-Smith G. Identifying novel causes of cancers to enhance cancer prevention: New strategies are needed. *J Natl Cancer Inst.* 2022;114:353-360.
- Swanepoel B, Nitulescu GM, Olaru OT, Venables L, van de Venter M. Anti-cancer activity of a 5-aminopyrazole derivative lead compound (BC-7) and potential synergistic cytotoxicity with cisplatin against human cervical cancer cells. *Int J Mol Sci.* 2019;20:5559.
- Kloskowski T, Szeliski K, Krzeszowiak K, et al. Mumio (Shilajit) as a potential chemotherapeutic for the urinary bladder cancer treatment. *Sci Rep.* 2021;11:22614.
- Campoccia D, Ravaoli S, Santi S, et al. Exploring the anticancer effects of standardized extracts of poplar-type propolis: In vitro cytotoxicity toward cancer and normal cell lines. *Biomedicine & Pharmacotherapy.* 2021;141:111895.
- Daina A, Michielin O, Zoete V. SwissTargetPrediction: updated data and new features for efficient prediction of protein targets of small molecules. *Nucleic Acids Res.* 2019;47:W357-W364.
- Zoete V, Daina A, Bovigny C, Michielin O. SwissSimilarity: A web tool for low to ultra high throughput ligand-based virtual screening. *J Chem Inf Model.* 2016;56:1399-1404.
- Gordon JL, Brown MA, Reynolds MM. Cell-based methods for determination of efficacy for candidate therapeutics in the clinical management of cancer. *Diseases.* 2018;6:85.
- Ligasová A, Frydrych I, Koberna K. Basic methods of cell cycle analysis. *Int J Mol Sci.* 2023;24:3674.
- Mani S, Swargiary G, Singh KK. natural agents targeting mitochondria in cancer. *Int J Mol Sci.* 2020;21:6992.
- Nakamura H, Takada K. Reactive oxygen species in cancer: Current findings and future directions. *Cancer Sci.* 2021;112:3945-3952.
- Chavda VP, Patel AB, Mistry KJ, et al. Nano-drug delivery systems entrapping natural bioactive compounds for cancer: recent progress and future challenges. *Front Oncol.* 2022;12:867655.
- Badmus JA, Ekpo OE, Hussein AA, Meyer M, Hiss DC. Cytotoxic and cell cycle arrest properties of two steroidal alkaloids isolated from *Holarthena floribunda* (G. Don) T. Durand & Schinz leaves. *BMC Complement Altern Med.* 2019;19:112.
- Duarte D, Nunes M, Ricardo S, Vale N. Combination of antimalarial and CNS drugs with antineoplastic agents in MCF-7 breast and HT-29 colon cancer cells: Biosafety evaluation and mechanism of action. *Biomolecules.* 2022;12:1490.
- Ren X, Yi Z, Sun Z, et al. Natural polysaccharide-incorporated hydroxyapatite as size-changeable, nuclear-targeted nanocarrier for efficient cancer therapy. *Biomater Sci.* 2020;8:5390-5401.
- Jiang Y, Wong S, Chen F, Chang T, Lu H, Stenzel MH. Influencing Selectivity to Cancer Cells with Mixed Nanoparticles Prepared from Albumin-Polymer Conjugates and Block Copolymers. *Bioconjug Chem.* 2017;28:979-985.
- Igoli NP, Obanu ZA, Gray AI, Clements C. Bioactive diterpenes and sesquiterpenes from the rhizomes of wild ginger (*Siphonochilus aethiopicus* (Schweinf) B.L. Burt). *Afr. J. Tradit., Complementary Altern. Med.* 2011;9:88-93.
- Lategan CA, Campbell WE, Seaman T, Smith PJ. The bioactivity of novel furanoterpenoids isolated from *Siphonochilus aethiopicus*. *J Ethnopharmacol.* 2009;121:92-97.

34. Li YW, Zhu GY, Shen XL, Chu JH, Yu ZL, Fong WF. Furanodienone inhibits cell proliferation and survival by suppressing ER α signaling in human breast cancer MCF-7 cells. *J Cell Biochem*. 2011;112:217-224.
35. Jänicke RU. MCF-7 breast carcinoma cells do not express caspase-3. *Breast Cancer Res Treat*. 2009;117:219-221.
36. Chen L, Liu YC, Zheng YY, et al. Furanodienone overcomes temozolomide resistance in glioblastoma through the downregulation of CSPG4-Akt-ERK signalling by inhibiting EGR1-dependent transcription. *Phytotherapy Research*. 2019;33:1736-1747.
37. Li YW, Zhu GY, Shen XL, Chu JH, Yu ZL, Fong WF. Furanodienone induces cell cycle arrest and apoptosis by suppressing EGFR/HER2 signaling in HER2-overexpressing human breast cancer cells. *Cancer Chemother Pharmacol*. 2011;68:1315-1323.
38. Jiang Y, Wang X, Hu D. Furanodienone induces G0/G1 arrest and causes apoptosis via the ROS/MapK-mediated caspase-dependent pathway in human colorectal cancer cells: A study in vitro and in vivo. *Cell Death Dis*. 2017;8:e2815.
39. Carneiro BA, El-Deiry WS. Targeting apoptosis in cancer therapy. *Nat Rev Clin Oncol*. 2020;17:395-417.
40. Perillo B, di Donato M, Pezone A, et al. ROS in cancer therapy: the bright side of the moon. *Exp Mol Med*. 2020;52:192-203.
41. Kim SJ, Kim HS, Seo YR. Understanding of ROS-inducing strategy in anticancer therapy. *Oxid Med Cell Longev*. 2019;2019:5381692.
42. Hasan A, Rizvi SF, Parveen S, Pathak N, Nazir A, Mir SS. Crosstalk between ROS and autophagy in Tumorigenesis: Understanding the multifaceted paradox. *Front Oncol*. 2022;12:852424.
43. Marullo R, Werner E, Degtyareva N, et al. Cisplatin induces a mitochondrial-ROS response that contributes to cytotoxicity depending on mitochondrial redox status and bioenergetic functions. *PLoS One*. 2013;8:e81162.
44. Ding Y, Wang H, Niu J, et al. Induction of ROS overload by alantolactone prompts oxidative DNA damage and apoptosis in colorectal cancer cells. *Int J Mol Sci*. 2016;17:558.
45. Rizzo A, Donzelli S, Girgenti V, et al. In vitro antineoplastic effects of brivaracetam and lacosamide on human glioma cells. *J. Exp. Clin. Cancer Res*. 2017;36:76.
46. Noel MS, Kim S, Hartley ML, et al. A randomized phase II study of SM-88 plus methoxsalen, phenytoin, and sirolimus in patients with metastatic pancreatic cancer treated in the second line and beyond. *Cancer Med*. 2022;11:4169-4181.
47. Anh NH, Kim SJ, Long NP, et al. Ginger on Human Health: A Comprehensive Systematic Review of 109 Randomized Controlled Trials. *Nutrients*. 2020;12:157.
48. Mahomoodally MF, Aumeeruddy MZ, Rengasamy KRR, et al. Ginger and its active compounds in cancer therapy: From folk uses to nano-therapeutic applications. *Semin Cancer Biol*. 2021;69:140-149.
49. Bernard MM, McConery JR, Hoskin DW. [10]-Gingerol, a major phenolic constituent of ginger root, induces cell cycle arrest and apoptosis in triple-negative breast cancer cells. *Exp Mol Pathol*. 2017;102:370-376.
50. Erasmus M, du Plessis LH, Viljoen JM. In-vitro cytotoxicity of various *Siphonochilus aethiopicus* (Schweinf.) B.L. Burt extracts in combination with selected tableting excipients. *J. Pharm. Pharmacol*. 2019;71:1714-1724.

SUPPORTING INFORMATION

Additional supporting information can be found online in the Supporting Information section at the end of this article.

How to cite this article: Ortigosa-Palomo A, Fuentes-Ríos D, Quiñero F, et al. Evaluation of cytotoxic effect of siphonochilone from African ginger: an *in vitro* analysis. *Environmental Toxicology*. 2024;1-14. doi:10.1002/tox.24308